MDC1 directs chromosome-wide silencing of the sex chromosomes in male germ cells

Yosuke Ichijima,[1,2] Misako Ichijima,[1,2] Zhenkun Lou,[3] André Nussenzweig,[4] R. Daniel Camerini-Otero,[5] Junjie Chen,[6] Paul R. Andreassen,[2,7] and Satoshi H. Namekawa[1,2,8]

[1]Division of Reproductive Sciences, Perinatal Institute, Cincinnati Children's Hospital Medical Center, Cincinnati, Ohio 45229, USA; [2]Department of Pediatrics, University of Cincinnati College of Medicine, Cincinnati, Ohio 45229, USA; [3]Division of Oncology Research, Department of Oncology, Mayo Clinic, Rochester, Minnesota 55905, USA; [4]Experimental Immunology Branch, National Cancer Institute, National Institutes of Health, Bethesda, Maryland 20892, USA; [5]Genetics and Biochemistry Branch, National Institute of Diabetes and Digestive and Kidney Diseases (NIDDK), National Institutes of Health, Bethesda, Maryland 20892, USA; [6]Department of Experimental Radiation Oncology, University of Texas M.D. Anderson Cancer Center, Houston, Texas 77030, USA; [7]Division of Experimental Hematology and Cancer Biology, Cincinnati Children's Hospital Medical Center, Cincinnati, Ohio 45229, USA

Chromosome-wide inactivation is an epigenetic signature of sex chromosomes. The mechanism by which the chromosome-wide domain is recognized and gene silencing is induced remains unclear. Here we identify an essential mechanism underlying the recognition of the chromosome-wide domain in the male germline. We show that mediator of DNA damage checkpoint 1 (MDC1), a binding partner of phosphorylated histone H2AX (γH2AX), defines the chromosome-wide domain, initiates meiotic sex chromosome inactivation (MSCI), and leads to XY body formation. Importantly, MSCI consists of two genetically separable steps. The first step is the MDC1-independent recognition of the unsynapsed axis by DNA damage response (DDR) factors such as ataxia telangiectasia and Rad3-related (ATR), TOPBP1, and γH2AX. The second step is the MDC1-dependent chromosome-wide spreading of DDR factors to the entire chromatin. Furthermore, we demonstrate that, in somatic cells, MDC1-dependent amplification of the γH2AX signal occurs following replicative stress and is associated with transcriptional silencing. We propose that a common DDR pathway underlies both MSCI and the response of somatic cells to replicative stress. These results establish that the DDR pathway centered on MDC1 triggers epigenetic silencing of sex chromosomes in germ cells.

[*Keywords*: germ cells; meiosis; meiotic sex chromosome inactivation; DNA damage response; MDC1; γH2AX]

Supplemental material is available for this article.

Received January 7, 2011; revised version accepted March 14, 2011.

Sex chromosomes are representative models of epigenetic gene regulation in which transcription is regulated in a chromosome-wide manner during development. In mammalian females, one of the X chromosomes is inactivated to equalize the X-linked gene dosage between XX females and XY males. For female X-inactivation, placental mammals, including humans and mice, acquired a noncoding RNA (*Xist*) that decorates an entire X chromosome to initiate chromosome-wide gene silencing (Chow and Heard 2010; Lee 2010). Another form of X inactivation occurs in male germ cells. During male meiosis, X and Y chromosomes are specifically silenced in a process called meiotic sex chromosome inactivation (MSCI). MSCI is an indispensable step in spermatogenesis. In contrast to female X inactivation, male MSCI is known to be *Xist*-independent (McCarrey et al. 2002; Turner et al. 2002). Despite previous studies that have implicated DNA damage response (DDR) factors in MSCI (Turner 2007; Inagaki et al. 2010), it remains unclear how the sex chromosomes are recognized and how gene silencing occurs in a chromosome-wide manner in male germ cells.

Germ cells faithfully transmit life's identity to the next generation and confer genetic diversity. During meiosis, homologous chromosomes undergo synapsis and recombination, leading to genetically variable gametes. In contrast, heterologous chromatins (such as sex chromosomes) are epigenetically silenced during meiosis in various organisms—including the fungus *Neurospora*, *Caenorhabditis elegans*, *Drosophila*, birds, and mammals—although the underlying mechanisms depend on the species (Kelly and Aramayo 2007; Namekawa and Lee 2009). Meiotic silencing of unsynapsed chromatin (MSUC) is thought to

[8]**Corresponding author.**
E-MAIL satoshi.namekawa@cchmc.org; FAX (513) 803-1160.
Article is online at http://www.genesdev.org/cgi/doi/10.1101/gad.2030811.

be an ancient fundamental mechanism designed to suppress heterologous unsynapsed chromatin (Baarends et al. 2005; Turner et al. 2005). This trait may have evolved as a genome defense mechanism to protect the host genome from invasion by external DNA, such as transposons (Huynh and Lee 2005; Kelly and Aramayo 2007). In the mammalian male germline, meiotic silencing is confined to the X and Y chromosomes (which are heterologous and largely unsynapsed) and manifests as MSCI (McKee and Handel 1993; Turner 2007; Namekawa and Lee 2009; Yan and McCarrey 2009; Inagaki et al. 2010).

Cytological evidence suggests that various DDR factors accumulate at sites of heterologous X and Y chromosomes. First, ataxia telangiectasia and Rad3-related (ATR) kinase, TOPBP1 (an ATR activator), and BRCA1 accumulate on the unsynapsed axis of the sex chromosome (Scully et al. 1997; Moens et al. 1999; Perera et al. 2004; Reini et al. 2004; Turner et al. 2004). Second, phosphorylation of H2AX (γH2AX) marks entire sex chromosomes at the onset of MSCI (Mahadevaiah et al. 2001). Previous studies suggest that, during MSCI, γH2AX occurs independently of ataxia telangiectasia-mutated (ATM) kinase but is dependent on ATR kinase (Turner et al. 2004; Bellani et al. 2005). ATR is known to sense ssDNA at the site of DNA damage in somatic cells (Cimprich and Cortez 2008; Friedel et al. 2009). H2AX knockout mice cannot induce MSCI and meiotic progression is arrested, suggesting the importance of H2AX in MSCI (Fernandez-Capetillo et al. 2003). However, genetic evidence is lacking to ascertain whether phosphorylation of H2AX and the associated DDR pathway are essential for MSCI.

To uncover the molecular mechanism underlying MSCI, we focused attention on mediator of DNA damage checkpoint 1 (MDC1), a binding partner of γH2AX. MDC1 plays a crucial role in the DDR signaling pathway downstream from γH2AX in somatic cells (Goldberg et al. 2003; Lou et al. 2003; Stewart et al. 2003). In this study, we show that MDC1 is an essential factor for the recognition of the chromosome-wide domain of meiotic sex chromosomes in male mice, and MDC1 is therefore indispensable in the establishment of MSCI and the XY body. Importantly, our studies in *Mdc1* knockout mice reveal that MSCI is genetically separable into two steps: MDC1-independent chromosome axis recognition and MDC1-dependent chromosome-wide domain formation. Herein we identify a novel mechanism of chromosome-wide regulation based on *cis*-recognition. Furthermore, the DDR pathway has a shared role in both MSCI and the somatic response to replicative stress during S phase. These results establish that the DDR pathway, centered on MDC1, recognizes chromosome-wide domains and induces epigenetic silencing of sex chromosomes in germ cells.

Results

MDC1 is essential for chromosome-wide spreading of γH2AX

To test the role of MDC1 in MSCI, we examined the phenotype of $Mdc1^{-/-}$ mice in male spermatogenesis. A previous study revealed male-specific infertility in $Mdc1^{-/-}$ mice due to meiotic arrest, whereas $Mdc1^{-/-}$ females are fertile, suggesting a critical role for MDC1 in a male-specific event in meiosis (Lou et al. 2006). A subsequent study confirmed that spermatogenesis in $Mdc1^{-/-}$ mice is arrested at epithelial stage IV, which corresponds to the mid-pachytene stage in normal meiosis (Ahmed et al. 2007). Consistent with previous studies, we did not observe abnormalities in $Mdc1^{-/-}$ mice before entry into meiosis (Supplemental Fig. S1) and spermatids were not observed in $Mdc1^{-/-}$ males, indicating that MDC1 is indispensable in male meiosis.

To further investigate the role of MDC1 in meiosis, we examined meiotic chromosome spreads of $Mdc1^{-/-}$ mice. In the leptotene and zygotene stages, when homologous chromosomes undergo synapsis following meiosis-specific DNA double-strand breaks (DSBs), the first wave of γH2AX accumulation occurred extensively in $Mdc1^{-/-}$ nuclei, as in the control (Supplemental Fig. S2). After the early pachytene stage in normal meiosis, when homologous synapsis is completed, γH2AX localized on the chromosome-wide domain of the sex chromosomes (Fig. 1A). However, in $Mdc1^{-/-}$ spermatocytes, chromosome-wide accumulation of γH2AX on sex chromosomes was significantly impaired at the pachytene stage, and the γH2AX signal was confined to the unsynapsed axis and proximal regions of sex chromosomes (Fig. 1B). This phenotype was observed in all $Mdc1^{-/-}$ pachytene spermatocytes that we examined, and spermatid progression to later stages totally failed ($n > 100$), indicating that sex chromosome-wide accumulation of γH2AX is a critical step in meiotic progression. However, it is also possible that the γH2AX-spreading defect in $Mdc1^{-/-}$ spermatocytes is caused indirectly by meiotic arrest during the course of γH2AX spreading. To test this possibility, we examined meiotic progression by staining a testis-specific histone variant (H1t) that specifically accumulates after the mid-pachytene stage, when MSCI is already established in normal meiosis (Inselman et al. 2003). We confirmed that $Mdc1^{-/-}$ germ cells can reach the H1t-positive stage, correlating with the mid-pachytene stage. Since the spreading defect is evident in H1t-positive cells (Supplemental Fig. S1), our results suggest that this defect is not the indirect consequence of meiotic arrest. Thus, we conclude that MDC1 is an essential factor for spreading γH2AX from the axes to the chromosome-wide domain of sex chromosomes in the pachytene stage.

Next, we examined the localization of ATR and TOPBP1 (ATR activator), which are thought to form a protein complex and be involved in phosphorylation of H2AX during MSCI (Turner et al. 2004; Bellani et al. 2005). In normal meiosis, during the zygotene-to-pachytene transition, ATR and TOPBP1 initially accumulated on the unsynapsed axes of sex chromosomes and then spread onto the chromosome-wide domain of the sex chromosomes (Fig. 1C,E). Intriguingly, in $Mdc1^{-/-}$ spermatocytes, the spreading of ATR and TOPBP1 from the unsynapsed axes to the chromosome-wide domain of the sex chromosomes was not observed, and the signals existed only on the unsynapsed axes (Fig. 1D,F). These results suggest that MDC1 is

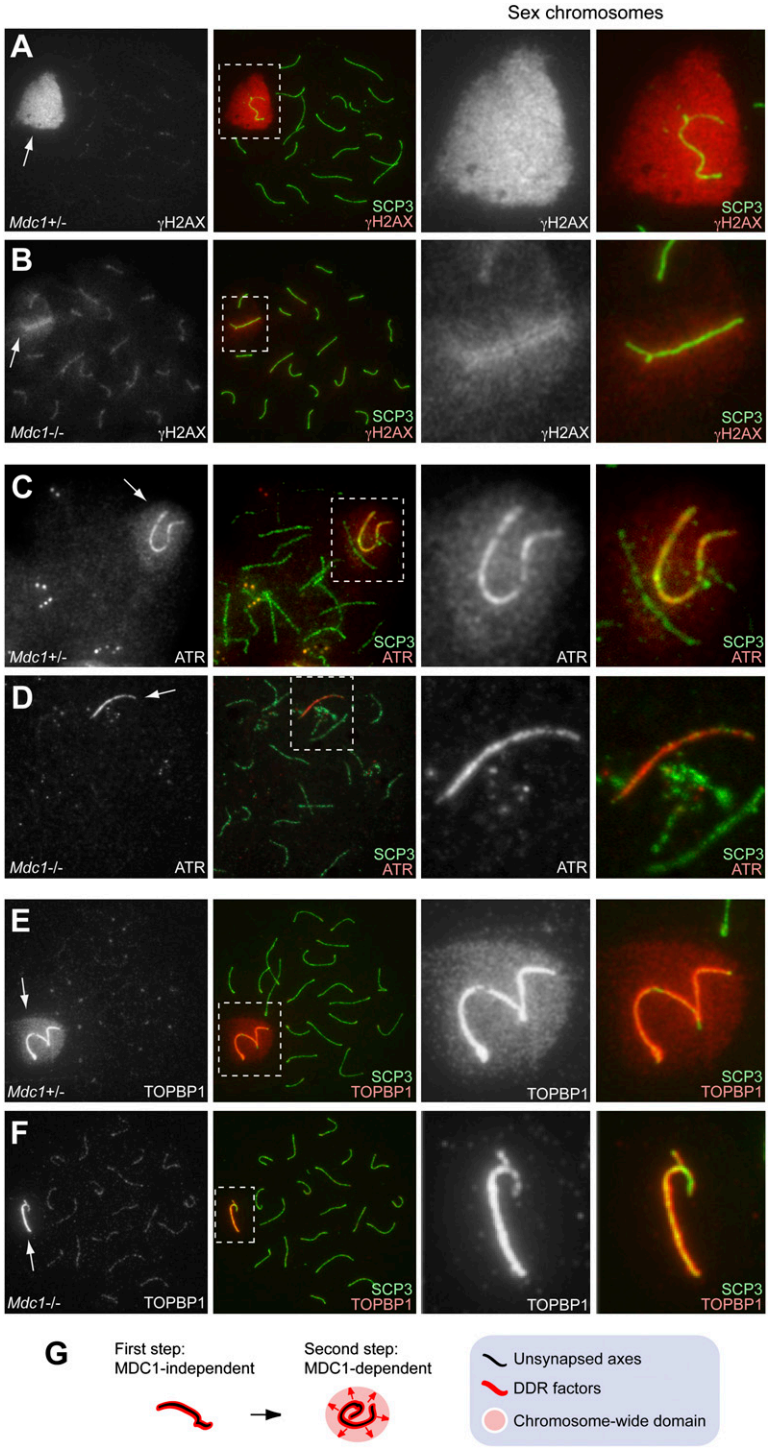

Figure 1. MDC1 directs chromosome-wide spreading of DDR factors. (*A–F*) Immunostaining of meiotic chromosome spreads using antibodies against DDR factors together with the anti-SCP3 antibody. SCP3 staining displays the status of chromosome synapsis and is used to distinguish meiotic stages. All images are wide-field images of pachytene spermatocytes. Areas surrounding sex chromosomes are highlighted in dotted rectangles and are magnified in the *right* panels. (Arrows) Sex chromosomes. (*G*) Pictorial representation about the role of MDC1 in MSCI. The first step is MDC1-independent recognition of the unsynapsed axis. The second step is MDC1-dependent spreading of DDR factors to the chromosome-wide domain.

an essential factor needed to build up chromosome-wide spreading of ATR and TOPBP1, as well as γH2AX. On the contrary, localization of BRCA1 was not altered in *Mdc1*$^{-/-}$ spermatocytes and was confined to the unsynapsed axes of sex chromosomes, as in controls (Supplemental Fig. S3). This suggests that BRCA1 does not function downstream from MDC1 during MSCI. Supporting its role in chromosome-wide spreading of DDR factors, MDC1 spreads onto the chromosome-wide domain in normal pachytene spermatocytes (Supplemental Fig. S3; Lee et al. 2005). Taken together, we conclude that MSCI consists of two genetically separable steps. The first step is the MDC1-independent recognition of the unsynapsed axis, in which the ATR–TOPBP1 complex phosphorylates H2AX (Fig. 1G). The second step is the MDC1-dependent chromosome-wide spreading of

the ATR–TOPBP1 complex and the γH2AX signal to the entire chromatin (Fig. 1G).

In addition to these factors, various DDR factors are known to accumulate on the sex chromosomes at the onset of MSCI. Mre11, Rad50, and Nbs1 form the multimeric MRN complex and accumulate at sites of DNA DSBs in somatic cells following γH2AX foci formation (Furuta et al. 2003). The MRN complex also accumulates on the chromosome-wide domain of the sex chromosomes during MSCI (Supplemental Fig. S4; Eijpe et al. 2000). To dissect the genetic pathway that MDC1 is involved in, we examined the localization of the MRN complex in *Mdc1*$^{-/-}$ spermatocytes. Mre11 and Rad50 localized on the unsynapsed axes of sex chromosomes in *Mdc1*$^{-/-}$ spermatocytes (Supplemental Fig. S4). This indicates that recruitment of the MRN complex to the unsynapsed axes is MDC1-independent, but that MDC1 is required for spreading of the MRN complex to the sex chromosome-wide domain. Although the function of the MRN complex in MSCI is unknown, these results further corroborate the essential role of MDC1 in the recognition of the chromosome-wide domain of the sex chromosomes by DDR factors during MSCI.

MDC1 initiates MSCI

To determine whether MDC1-dependent chromosome-wide recognition is needed for transcriptional silencing of the sex chromosomes, we examined the general transcriptional status by immunostaining using an antibody against RNA polymerase II (Pol II). We prepared meiotic slides using a method we developed previously to conserve the morphology of meiotic chromatin and the three-dimensional nuclear structure (Namekawa et al. 2006; Namekawa and Lee 2011). In normal pachynema, the sex chromosomes formed a silent compartment, called the XY body, in which Pol II was largely excluded from the entire sex chromosome (Fig. 2A,C; Namekawa et al. 2006). In *Mdc1*$^{-/-}$ pachynema, the unsynapsed axes of sex chromosomes were located largely in the transcriptionally active euchromatic region, except for the centromeric end of the X chromosome and a large part of the Y chromosome that is known to reside in silent heterochromatin even before meiosis (Fig. 2B,D; Namekawa et al. 2006). We conclude that MDC1 is required for establishing chromosome-wide silencing. This conclusion was confirmed independently by Cot-1 RNA fluorescent in situ hybridization (FISH). Cot-1 DNA consists of repetitive elements that can hybridize to nascent transcripts, leading to visible transcriptionally active regions (Hall et al. 2002). The Cot-1 signal was similarly excluded from the XY in the control, as was the case for Pol II staining (Fig. 2E). In contrast, the unsynapsed axes of sex chromosomes were located in the Cot-1-positive region in *Mdc1*$^{-/-}$ spermatocytes (Fig. 2F) despite the fact that various DDR factors accumulated on

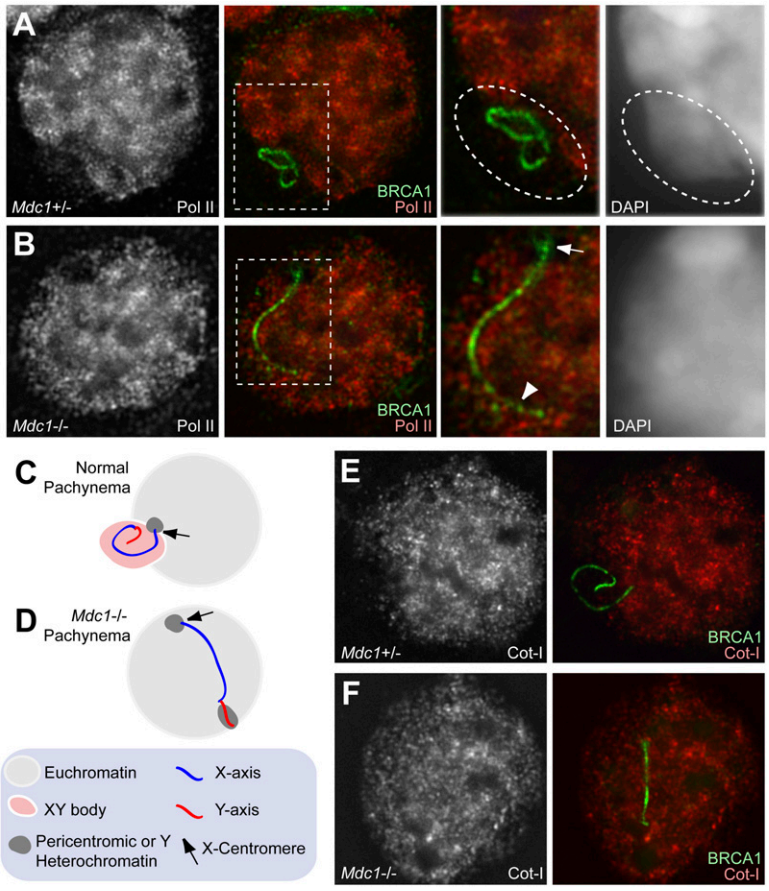

Figure 2. MDC1 is required for MSCI. (*A*,*B*) Immunostaining with anti-Pol II antibody in *Mdc1*$^{+/-}$ and *Mdc1*$^{-/-}$ spermatocytes, respectively. Unsynapsed axes of sex chromosomes are detected with anti-BRCA1 antibody. Areas surrounding sex chromosomes are highlighted in dotted rectangles and are magnified in the *right* panels. The outline of the XY body is highlighted with a dotted oval. (Arrow) Centromeric end of the X chromosome; (arrowhead) Y-chromosome part of the sex chromosome pair. (*C*,*D*) Pictorial representation of the unsynapsed axes of sex chromosomes. (*E*,*F*) Combined immunostaining with anti-BRCA1 antibody and Cot-1 RNA FISH in *Mdc1*$^{+/-}$ and *Mdc1*$^{-/-}$ cells, respectively. Meiotic slides were prepared as described (Namekawa et al. 2006). All images are deconvolved single *Z*-sections.

the axes (Fig. 1). This suggests that the chromatin conformational change following DDR factor accumulation is required for transcriptional silencing.

To confirm these cytological analyses, we performed microarray analysis using Affymetrix Gene 1.0 ST arrays to examine gene expression profiles in juvenile testes in which the first wave of meiosis is semisynchronous. For example, the pachytene stage commences at ~10 d after birth. At 16.5 d old, when MSCI is already established in normal meiosis, genes on the sex chromosomes were not repressed and were consequently up-regulated in *Mdc1*$^{-/-}$ testes as compared with wild-type testes (Fig. 3A). We also examined average expression levels in individual chromosomes and confirmed that up-regulation in *Mdc1*$^{-/-}$ testes is specific to the sex chromosomes (Fig. 3B). Up-regulation of the X chromosome in *Mdc1*$^{-/-}$ testes occurs in a chromosome-wide manner (Fig. 3C). We conclude that MDC1-dependent recognition of the chromosome-wide domain is a critical step in the initiation of chromosome-wide silencing in MSCI.

MDC1 is required for XY body formation

The chromosome-wide accumulation of γH2AX on sex chromosomes is concomitant with the formation of a distinct heterochromatin domain called the XY body (also known as sex body). Various epigenetic modifications, including histone modifications, occur specifically on the XY body following its formation (Greaves et al. 2006; Namekawa et al. 2006; Turner et al. 2006; van der Heijden et al. 2007). The XY body is a distinct chromatin domain detected by characteristic DAPI staining, as shown in Figure 2A. The MSCI defect in *Mdc1*$^{-/-}$ spermatocytes suggests that MDC1 is essential for the formation of this distinct chromatin domain. To determine whether XY body formation depends on MDC1, we examined localization of various XY body markers. Sumoylation occurs on entire sex chromosomes in normal meiosis (Fig. 4A; Rogers et al. 2004), but was completely abolished in *Mdc1*$^{-/-}$ spermatocytes (Fig. 4B). Although a previous observation suggested that SUMO-1 accumulation precedes γH2AX on the XY body (Vigodner 2009), our genetic evidence demonstrates unequivocally that γH2AX–MDC1 signaling is upstream of SUMO-1 accumulation in both the axes and the chromosome-wide domain of the sex chromosomes. Consistent with this result, a recent study revealed that SUMO proteins function downstream from the DDR pathway in somatic cells (Galanty et al. 2009). Furthermore, various XY body markers—such as Xmr (Escalier and Garchon 2000), MacroH2A1 (Hoyer-Fender et al. 2000), ubiquitin conjugates (FK2), and ubiquitinated histone H2A (Ubi-H2A) (Baarends et al. 2005)—did not localize on chromosome-wide domains on the sex chromosome in *Mdc1*$^{-/-}$ cells (Fig. 4C–J). Axial accumulation of Xmr, MacroH2A, and Ubi-H2A was observed in *Mdc1*$^{-/-}$ cells, however. Exclusion of histone H3 trimethylated at Lys 27 (H3K27me3) was also MDC1-dependent (Fig. 4K,L). Taken together, we establish that γH2AX–MDC1 signaling precedes chromosome-wide accumulation of various XY body markers and confers chromosome-wide epigenetic alterations on the sex chromosomes.

We further investigated the chromatin conformation of sex chromosomes by directly measuring the degree of compaction of the XY chromosome axes. For this purpose, we quantified the distance between the distal ends of the XY axes displayed by BRCA1 staining (Fig. 4M,N). As illustrated in Figure 4M, sex chromosome axes in *Mdc1*$^{-/-}$ pachynema were stretched longer than those in normal spermatocytes in both early and mid-pachytene stages (Fig. 4N). These results demonstrate that MDC1 directs the chromatin conformational change of sex chromosomes at the early pachytene stage, concomitant with the establishment of MSCI, leading to establishment of the XY body.

Meiotic recombination in Mdc1$^{-/-}$ *mice*

DDR factors, including γH2AX and MDC1, also accumulate in autosome regions at the leptotene and zygotene stages (Mahadevaiah et al. 2001; Lee et al. 2005) when meiosis-specific DSBs are induced by Spo11 to initiate

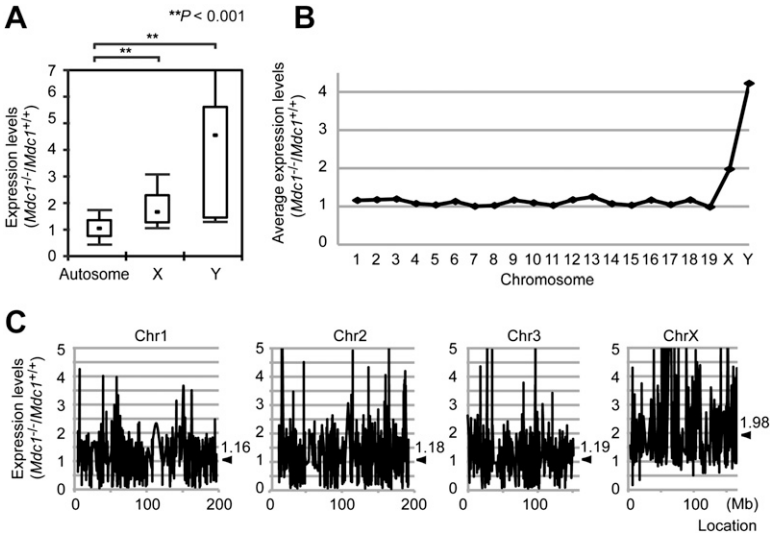

Figure 3. Microarray analysis of *Mdc1*$^{-/-}$ testis at 16.5 d old. (*A*) Comparison of gene expression levels in *Mdc1*$^{-/-}$ versus *Mdc1*$^{+/+}$ cells among autosomes or X and Y chromosomes. The central dot is the median, the boxes encompass 50% of data points, and the error bars indicate 90% of data points. *P* was derived from a paired *t*-test. (*B*) Average expression levels in *Mdc1*$^{-/-}$ versus *Mdc1*$^{+/+}$ mice for each chromosome. (*C*) Expression levels along the location of representative autosomes (Chr1–Chr3) and the X chromosome. Locations are distances from proximal ends of chromosomes (in megabases). Arrowheads denote average expression levels in each chromosome.

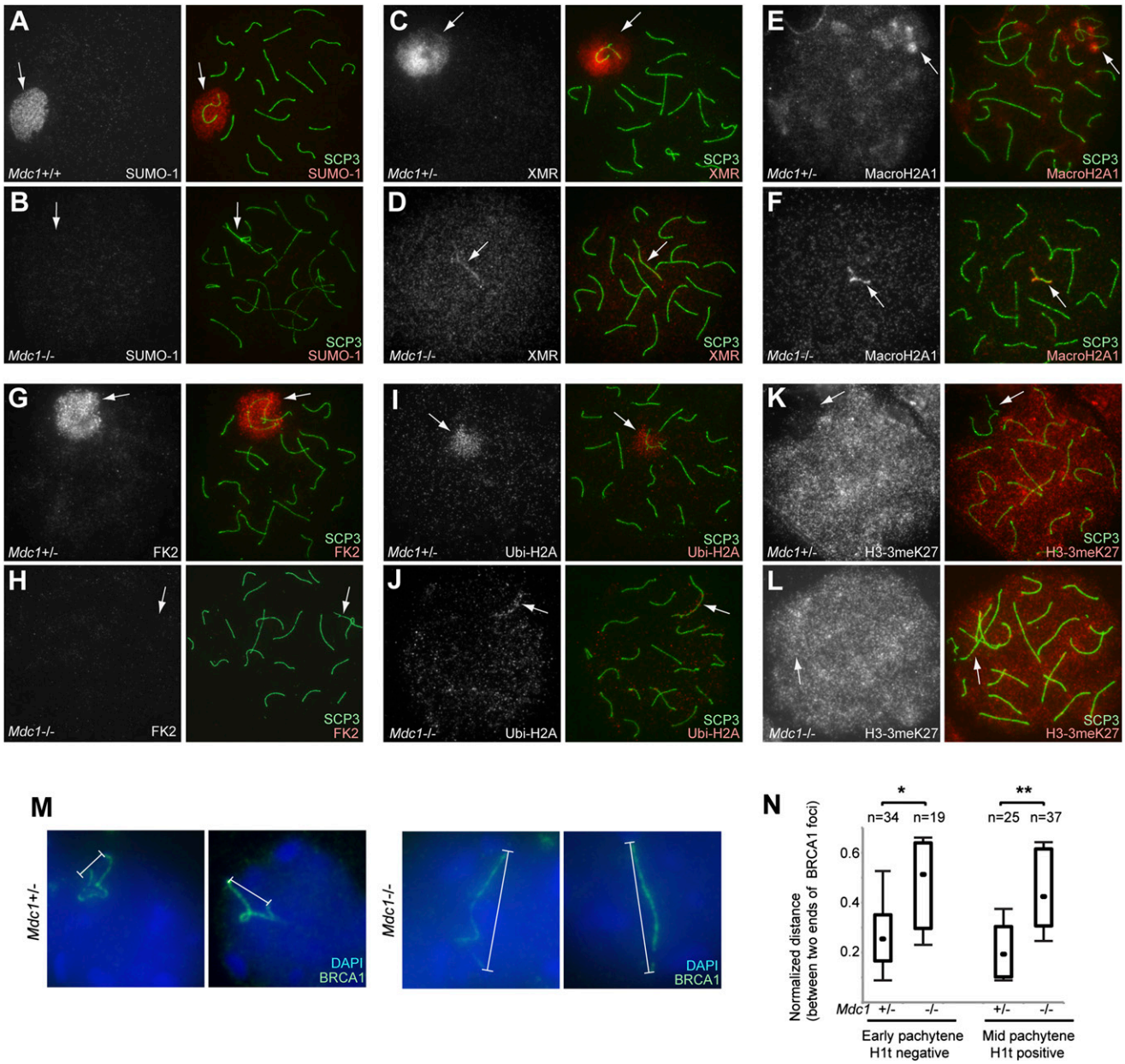

Figure 4. γH2AX–MDC1 signaling is the primary step in XY body formation. (*A–L*) Immunostaining of meiotic chromosome spreads using the indicated antibodies together with the anti-SCP3 antibody. All pictures represent pachytene spermatocytes. (Arrows) Sex chromosomes. All images are wide-field images. (*M*) Conformation of sex chromosome axes detected by BRCA1 staining in pachytene $Mdc1^{+/-}$ and $Mdc1^{-/-}$ spermatocytes. To preserve relative three-dimensional conformation, meiotic slides were prepared as described (Namekawa et al. 2006). (*N*) Summary of linear distances between both ends of sex chromosome axes. The normalized distance is the linear distance between both ends detected with BRCA1 staining normalized to the nuclear diameter. The central dot is the median, the boxes encompass 50% of data points, and the error bars indicate 90% of data points. Meiotic stages were judged by simultaneous staining with SCP3 and H1t. *P*-values were calculated using an unpaired *t*-test. (*) $P < 0.01$; (**) $P < 0.001$.

meiotic recombination (Baudat et al. 2000; Romanienko and Camerini-Otero 2000). This meiotic recombination is tightly associated with the progression of homologous chromosome synapsis. Intriguingly, γH2AX and TOPBP1 foci remained along autosome axes in $Mdc1^{-/-}$ pachytene spermatocytes, but decreased on autosome axes in normal meiosis (Fig. 1). If MDC1 has a role in processing meiotic DSBs at the leptotene and zygotene stages, it could indirectly disturb meiotic silencing at the subsequent pachytene stage in $Mdc1^{-/-}$ mice. To distinguish the roles of MDC1 in meiotic silencing and recombination, we characterized the roles of MDC1 in meiotic recombination using $Mdc1^{-/-}$ mice. We first examined chromosome synapsis, which is tightly associated with the initiation of meiotic recombination in mice (Baudat et al. 2000; Romanienko and Camerini-Otero 2000). We found normal

synapsis of *Mdc1*$^{-/-}$ autosomes at the pachytene stage (n = 70), as judged by immunostaining of SCP1, which localizes only on synapsed chromosomes (Fig. 5A,B). This suggests that MDC1 is not required for the initial stage of meiotic recombination. However, *Mdc1*$^{-/-}$ spermatocytes exhibited sex chromosome-specific synaptic defects, X and Y axes that were not associated (14%, n = 70) (Fig. 5C), and illegitimate association of an end of the X axis to autosomes (24%, n = 70) (Fig. 5D) at a higher frequency than in normal spermatocytes (both 0%, n = 50). These abnormalities are also observed in H2AX knockout mice (Celeste et al. 2002; Fernandez-Capetillo et al. 2003), suggesting the crucial role of γH2AX–MDC1 signaling in sex chromosome synapsis.

To examine the phenotype in terms of processing meiotic DSBs in *Mdc1*$^{-/-}$ spermatocytes, we examined the localization of recombination intermediates by immunofluorescence with marker antibodies such as RAD51, RPA, and MLH1 (Plug et al. 1998; Tarsounas et al. 1999). RAD51 accumulated at sites of DSBs and subsequent strand invasion during meiotic recombination in the leptotene and zygotene stages in controls (Fig. 5E). After processing of recombination intermediates at the pachytene stage, RAD51 disappeared from autosomal axes and remained only on the X axis (Fig. 5G; Plug et al. 1998). In *Mdc1*$^{-/-}$ spermatocytes, localization of RAD51 foci was indistinguishable from that in normal spermatocytes (Fig. 5F,H). Next we examined the localization of RPA, an ssDNA-binding protein that marks synapsed regions at the site of recombination after the zygotene stage. RPA is a late marker of recombination intermediates, after RAD51 accumulation (Fig. 5I; Plug et al. 1998). In *Mdc1*$^{-/-}$ spermatocytes, RPA foci formation occurred normally, suggesting normal processing of meiotic DSBs (Fig. 5J). However, the localization of MLH1, which marks one or two sites of crossover recombination in normal meiosis (Fig. 5K; Baker et al. 1996), was completely abolished in *Mdc1*$^{-/-}$ spermatocytes (Fig. 5L). These results in *Mdc1*$^{-/-}$ spermatocytes raised two possibilities: that MDC1 has a direct role in processing crossover recombination and promoting MLH1 accumulation, or that an MSCI defect causes meiotic arrest at the stage before MLH1 accumulation and indirectly impedes MLH1 accumulation on autosomes.

To address these two possibilities, we examined the recombination intermediates in *Mdc1*$^{-/-}$ female meiosis. Consistent with normal fertility in female *Mdc1*$^{-/-}$ mice, we observed normal accumulations of RPA and MLH1

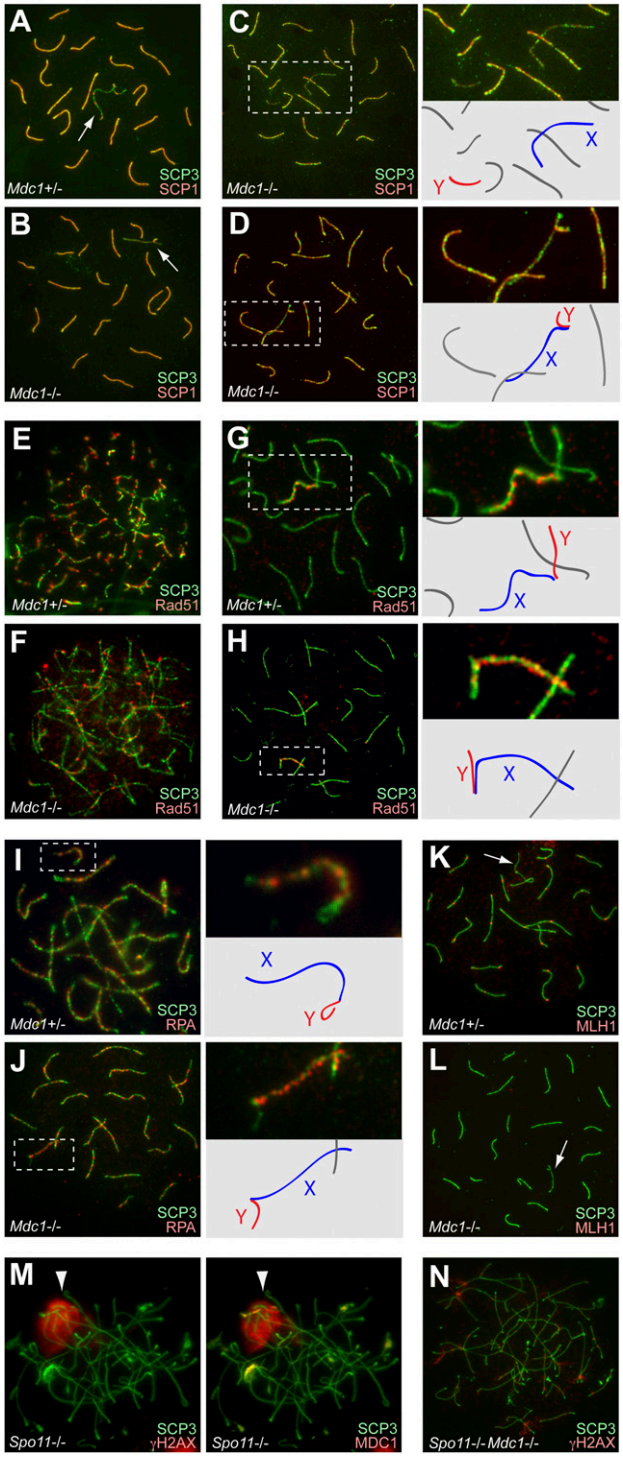

Figure 5. Meiotic recombination in the *Mdc1* mutant. Immunostaining of meiotic chromosome spreads using the indicated antibodies together with the anti-SCP3 antibody. All images are wide-field images. (Arrows) Sex chromosomes. (*A*,*B*) Chromosome synapsis occurs normally at the pachytene stage in *Mdc1*$^{+/-}$ and *Mdc1*$^{-/-}$ spermatocytes. (*C*) *Mdc1*$^{-/-}$ spermatocytes exhibit sex chromosome-specific synaptic defects. (*D*) Illegitimate associations of the X axis to autosomes in *Mdc1*$^{-/-}$ spermatocytes. Areas surrounding sex chromosomes (dotted rectangle) are magnified in the *right* panels, and schematics of chromosome axes are shown *below*. (*E*,*F*) Rad51 foci formation is normal at the zygotene stage in *Mdc1*$^{+/-}$ and *Mdc1*$^{-/-}$ spermatocytes. (*G*,*H*) Rad51 foci disappear from autosomal regions and remain only on the X-chromosome axis at the pachytene stage in *Mdc1*$^{+/-}$ and *Mdc1*$^{-/-}$ spermatocytes. (*I*,*J*) RPA foci formation is normal at the pachytene stage in *Mdc1*$^{+/-}$ and *Mdc1*$^{-/-}$ spermatocytes. (*K*) MLH1 marks the sites of crossover at the pachytene stage in *Mdc1*$^{+/-}$ spermatocytes. (*L*) MLH1 foci are abolished in *Mdc1*$^{-/-}$ at the pachytene stage. (*M*) MDC1 localizes on the pseudo sex body in *Spo11*$^{-/-}$ spermatocytes. (Arrowhead) Pseudo sex body. (*N*) The pseudo sex body is abolished in spermatocytes of the *Spo11*$^{-/-}$*Mdc1*$^{-/-}$ double mutant.

foci in *Mdc1*$^{-/-}$ females (Supplemental Fig. S5). These results support the latter possibility that an MSCI defect causes meiotic arrest and indirectly abolishes MLH1 foci in *Mdc1*$^{-/-}$ spermatocytes.

A role for MDC1 in meiotic silencing independent of meiotic recombination

As further support for MDC1 function in meiotic silencing independent of meiotic recombination, we examined the *Spo11* mutant (*Spo11*$^{-/-}$) that is defective in inducing meiosis-specific DSBs and exhibits aberrant synapsis and meiotic arrest. Interestingly, meiotic silencing characterized by the accumulation of DDR factors such as ATR and γH2AX still takes place in *Spo11*$^{-/-}$ spermatocytes. However, in this case, the region of meiotic silencing locates ectopically, rather than on sex chromosomes, presumably due to the aberrant synapsis of autosomes. This region is called the pseudo sex body (Barchi et al. 2005; Bellani et al. 2005; Mahadevaiah et al. 2008). These observations strongly suggest that meiotic silencing is a genetically separable event from meiosis-specific DSBs, although correct localization of silencing on sex chromosomes may be a consequence of homologous chromosome synapsis that is, in turn, strictly dependent on meiosis-specific DSBs. We found that MDC1 accumulated in the pseudo sex body in *Spo11*$^{-/-}$ spermatocytes and perfectly overlapped with γH2AX, which illuminates the pseudo sex body domain (Fig. 5M). Furthermore, pseudo sex body formation was abolished in spermatocytes of the the *Spo11*$^{-/-}$*Mdc1*$^{-/-}$ double mutant (Fig. 5N). We conclude that MDC1 is required for pseudo sex body formation and meiotic silencing, supporting the notion that MDC1 functions directly in meiotic silencing independently of meiotic recombination.

MDC1 functions independently of RNF8 in MSCI

Next we sought to determine the pathway associated with MDC1 in MSCI. In the somatic DDR pathway, MDC1 recruits an E3 ubiquitin ligase, ring finger protein 8 (RNF8), via a direct interaction, leading to the subsequent recruitment of various DDR factors to the site of DNA damage (Huen et al. 2007; Kolas et al. 2007; Mailand et al. 2007). We found that RNF8 also localized on the XY body, but that the accumulation of RNF8 occurred only after the late diplotene phase (Supplemental Fig. S6). This is much later than that of MDC1, suggesting that MDC1 and RNF8 operate independently in MSCI. To determine the role of RNF8 on the XY body, we examined the phenotype of *Rnf8* $^{-/-}$ spermatocytes. In *Rnf8* $^{-/-}$ spermatocytes, chromosome-wide accumulation of MDC1, TOPBP1, SUMO-1, and Xmr were not disturbed (Supplemental Fig. S6). This result is consistent with recent studies showing normal chromosome-wide accumulation of γH2AX on the sex chromosomes, while ubiquitin conjugates are abolished from the XY body in *Rnf8* $^{-/-}$ spermatocytes (Lu et al. 2010; Santos et al. 2010). We conclude that RNF8 is dispensable for sex chromosome-wide localization of DDR factors and accumulation of XY body markers (except for ubiquitin conjugates), and MDC1 functions independently of RNF8 in MSCI.

A common role for MDC1 in meiotic silencing and the DDR pathway after replicative stress in somatic cells

The above results establish that MDC1 works downstream from ATR and amplifies γH2AX signals in the chromosome-wide domain, which induces MSCI. Based on this conclusion, we hypothesized that a common DDR pathway underlies both meiotic silencing and the somatic DDR, and that MDC1 is a common central player in γH2AX amplification. We anticipated that transcriptional silencing is a common consequence of γH2AX amplification in both meiotic silencing and somatic DDR. Supporting our notion, it has been shown that MDC1 amplifies γH2AX signals at the site of DNA DSBs in somatic cells by a feedback loop with ATM kinase (Lou et al. 2006). However, it is unclear whether MDC1-dependent γH2AX amplification also occurs downstream from ATR signaling. In somatic DDR, replicative stress activates an ATR-dependent pathway, rather than ATM, at the site of the stalled replication fork in S phase (Cimprich and Cortez 2008; Friedel et al. 2009). To explore our hypothesis, we investigated the role of MDC1 in the ATR-dependent pathway after the induction of replicative stress in the U2OS human osteosarcoma cell line. We sought to determine whether MDC1 amplifies γH2AX signals after induction of replicative stress, and whether γH2AX foci are associated with transcriptional silencing, as is the case with meiotic silencing.

Replicative stress can be induced by treatment of cells with hydroxyurea (HU). We confirmed that HU treatment specifically induces γH2AX foci in S phase using 5-ethynyl-2′-deoxyuridine (EdU), which is incorporated into replicating cells (Fig. 6A). To determine the role of MDC1 in the ATR-dependent pathway, we performed siRNA-based knockdown of MDC1. Following MDC1 knockdown, we observed that γH2AX amplification was significantly hampered after HU treatment (Fig. 6B,C). We conclude that MDC1 is also necessary for γH2AX amplification in an ATR-dependent pathway of somatic cells. Therefore, we propose that MDC1 directs γH2AX amplification, possibly by a feedback loop with the ATR–TOPBP1 complex, in both meiotic silencing and the response of somatic cells to replicative stress (Fig. 6D).

To investigate whether γH2AX amplification in the somatic ATR-dependent pathway is associated with transcriptional silencing, we performed double immunostaining of Pol II and γH2AX after HU treatment. As shown in Figure 6E, sites of γH2AX accumulation after HU treatment were mutually exclusive from those of Pol II accumulation. In accord with our conclusion about the critical role of MDC1 in meiotic silencing, we establish that the common ATR-dependent pathway centered on MDC1 is associated with both meiotic silencing and transcriptional silencing following replicative stress.

Discussion

We demonstrate that MDC1 plays a critical role in chromosome-wide silencing of the sex chromosomes. However,

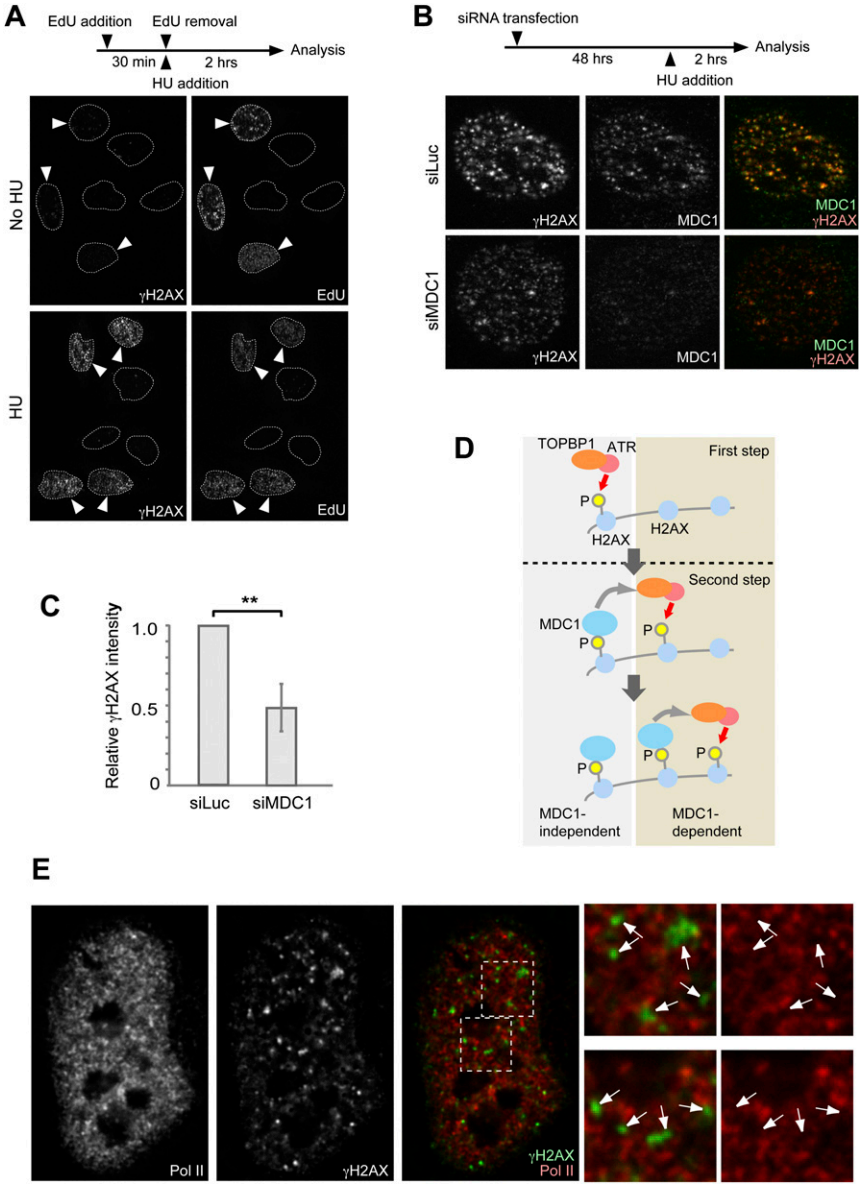

Figure 6. MDC1 amplifies γH2AX signal after replicative stress in somatic cells. (*A*) Replicative stress induction by HU and the appearance of γH2AX foci during S phase. U2OS cells were treated with 10 μM EdU for 30 min prior to 1 mM HU treatment for 2 h. Images are confocal images using Optiglid. (Arrowheads) S-phase cells. Dotted circles show nuclear regions. (*B*) γH2AX signal amplification is hampered by the knockdown of MDC1. U2OS cells were treated with siRNAs for 48 h prior to 1 mM HU treatment for 2 h. siRNA for luciferase gene (siLuc) was used as a negative control. Images are confocal images using Optiglid. (*C*) Quantification of γH2AX signal intensity after MDC1 knockdown. More than 30 nuclei of three independent experiments were examined, quantified using the ImageJ software, and normalized against the value of control siRNA (siLuc). *P* was derived from an unpaired *t*-test. The error bar shows standard deviation. (*D*) Model showing the role of MDC1 in γH2AX amplification. The first step is MDC1-independent induction of γH2AX. The second step is MDC1-dependent amplification of γH2AX signals in a feedback loop with TOPBP1 and ATR. MDC1 directs spreading of DDR factors to adjacent nucleosomes. (*E*) Foci of γH2AX and Pol II are mutually exclusive in U2OS cells after the 2-h HU treatment. Serial *Z*-sections were deconvolved and a representative *Z*-section is shown. Areas in dotted rectangles are magnified in the *right* panels. (Arrows) Sites of γH2AX foci.

it is likely that MDC1 is dispensable in meiotic recombination, which is a common event in both sexes, since *Mdc1*$^{-/-}$ females are fertile (Lou et al. 2006) and we do not see defects in autosomal synapsis or formation of early recombination intermediates in males. We show that *Mdc1*$^{-/-}$ germ cells can partially retain early markers of meiotic silencing (γH2AX, ATR, and TOPBP1) only on the axes of sex chromosomes. However, *Mdc1*$^{-/-}$ spermatocytes have defects in spreading these factors to the entire sex chromosome, in establishing the XY body, and in chromosome-wide gene silencing. A previous study suggests that MDC1 amplifies γH2AX by a feedback loop with the ATM kinase at the site of DSBs in somatic cells (Lou et al. 2006). Another study in somatic cells showed that γH2AX is dispensable for the initial recognition of DNA breaks but is required for amplification of DDR factors at DNA breaks (Celeste et al. 2003). Taken together, we propose that the initial γH2AX signal occurs at the unsynapsed axes of sex chromosomes in an MDC1-independent manner. MDC1 then mediates the spreading of the γH2AX signal over the chromosome-wide domain through a feedback loop with the ATR–TOPBP1 complex, thus leading to the recognition of the chromosome-wide domain and to XY body formation (Figs. 1G, 6D). In support of this model, a direct interaction between MDC1 and TOPBP1 has been identified in somatic cells following replicative stress (Wang et al. 2011). This finding strongly supports the possibility that MDC1 directly recruits the ATR–TOPBP1 complex to amplify the γH2AX signals in meiotic silencing (Fig. 6D), although other unidentified factors may also be involved in this process. The role of DDR factors in the recognition of the chromosome-wide domain is further supported by our data showing that XY body markers do not localize to the chromosome-wide domain of the sex chromosomes in male *Mdc1*$^{-/-}$ cells

during meiosis (Fig. 4). Thus, a DDR pathway centered on MDC1 is the critical determinant of chromosome-wide *cis* regulation of the sex chromosomes in MSCI.

Although a previous study demonstrated that deletion of the H2AX gene abolishes MSCI (Fernandez-Capetillo et al. 2003), it is unclear whether γH2AX is the cue that signals MSCI. In somatic cells, MDC1 binds to γH2AX to exert its function (Stewart et al. 2003). In this study, defective MSCI in *Mdc1*$^{-/-}$ mice provides compelling evidence that γH2AX is an essential signal for MSCI and XY body formation. Therefore, the current study provides the first genetic evidence that γH2AX and the associated DDR pathway are essential for MSCI.

DDR pathways mediate signaling downstream from DNA damage. Collapse of DDR pathways causes aberrant DNA repair, genomic instability, and predisposition to cancer (Andreassen and Niedernhofer 2009; Huen et al. 2010). We show that, in MSCI, recognition of the chromosome-wide domain by DDR factors takes place before the establishment of gene silencing and epigenetic modifications such as histone tail modifications. Surprisingly, our data suggest a common function for the DDR pathway and MDC1 in meiotic silencing and the response of somatic cells to DNA replication stress. It is well known that DNA replication stress stalls the replication fork in the mitotic S phase and that an ATR-dependent signaling cascade plays a central role in the DDR at the stalled replication fork (Cimprich and Cortez 2008; Friedel et al. 2009). A recent study revealed that an ATM-dependent pathway is associated with transcriptional silencing at the site of DNA DSBs in somatic cells (Shanbhag et al. 2010). Taken together, these results suggest that transcriptional silencing is a common consequence of γH2AX amplification in response to replication stress and DSBs mediated by ATR and ATM, respectively.

Notably, our data reveal a novel mechanism of chromosome-wide regulation. We propose that MDC1 establishes chromosome-wide silencing via signal amplification of γH2AX. Given that γH2AX foci are formed quite rapidly after induction of DNA damage in somatic cells, we suggest that the DDR pathway can provide an expeditious recognition of entire chromosomes during meiosis. These rapid kinetics during the initiation phase of MSCI are strikingly different from those of *Xist*-dependent X-chromosome inactivation in females. In both imprinted and random X inactivation, the noncoding RNA *Xist* gradually spreads and consequently establishes chromosome-wide genic silencing over several days (Okamoto et al. 2004; Chaumeil et al. 2006; Namekawa et al. 2010). The gradual establishment of female X inactivation may have enabled the regulation of several escape genes on a gene-by-gene basis, which eventually grew to be a relatively large number of escape genes in humans (such genes constitute ~15% of genes on human X chromosomes) (Carrel and Willard 2005). On the other hand, the rapid kinetics of male MSCI could explain why MSCI results in an almost complete shutdown of the X-linked genes, with the exception of only a few X-linked coding genes and many X-linked microRNA (miRNA) genes (Namekawa et al. 2006; Song et al. 2009).

What is the raison d'etre for DDR pathway-based recognition of the chromosome-wide domain in MSCI? Importantly, *Mdc1*$^{-/-}$ and *H2AX*$^{-/-}$ mice exhibit complete arrest with no progression of spermatocytes to the later stages (Fernandez-Capetillo et al. 2003; Lou et al. 2006). It has been proposed that suppression of sex-linked genes is essential in meiotic progression, and that the MSCI defect activates the meiotic checkpoint that leads to apoptotic elimination of germ cells (Burgoyne et al. 2009). The rapid kinetics of MSCI would support this view in that expeditious silencing is critical in checkpoint suppression and meiotic progression. Furthermore, in the course of evolution, DDR pathway-based MSCI also confers long-term benefits that would justify selection in favor of MSCI. Several theories consider the evolutionary benefits of MSCI to be suppression of illegitimate recombination between unsynapsed sex chromosomes (McKee and Handel 1993), protection from invasion of transposons (Huynh and Lee 2005; Kelly and Aramayo 2007), and acting as a driving force of transgenerational epigenetic inheritance (Huynh and Lee 2005; Namekawa et al. 2006, 2007). Future challenges will be to test the evolutionary history of sex chromosome inactivation and dissect the molecular mechanisms downstream from γH2AX–MDC1 signaling that confer transcriptional silencing and epigenetic memories on sex chromosomes.

Materials and methods

Mice

Mdc1, *Spo11*, and *Rnf8* mutants were on C57BL/6 backgrounds. For slide preparation, mutants and littermate controls were processed at 20–60 d of age, post-partum. For the microarray analysis, juvenile testes were processed at post-partum day 16.5. Embryos from *Mdc1*$^{-/-}$ females were obtained on embryonic day 17.5, after natural mating with *Mdc1* heterozygous males.

Spermatogenesis slide preparation

Hypotonic treatment was performed as described (Peters et al. 1997). Slides to conserve the morphology of meiotic chromatin and relative three-dimensional nuclear structures in mouse testes were prepared as described (Namekawa et al. 2006; Namekawa and Lee 2011). To prepare paraffin blocks, testes were fixed with 4% paraformaldehyde in PBS, ethanol-dehydrated, and embedded in paraffin. Six-micron paraffin sections were prepared with a microtome (Leica) and deparaffinized prior to immunostaining.

FISH and immunofluorescence

Cot-1 RNA FISH was performed as described (Namekawa and Lee 2011). For immunofluorescence, slides were incubated in PBT (0.15% BSA, 0.1% Tween 20 in PBS) for 60 min prior to overnight incubation at room temperature with the following antibodies: SCP3 (Novus), 1:100; Pol II CTD 8WG16 (Millipore), 1:200; H3-3meK27 (Millipore), 1:200; γH2AX (Millipore), 1:5000; ATR (Calbiochem), 1:400; TOPBP1 (generated by the Chen laboratory) (Yamane et al. 2002), 1:500; MDC1 (generated by the Nussenzweig laboratory), 1:500; SUMO-1 (Invitrogen), 1:400; XMR (gift from Denise Escalier), 1:500; macroH2A (Millipore), 1:200; ubiquitin conjugates (FK2, Enzo Life Sciences), 1:500; Ubi-H2A (Millipore), 1:200; H1t (gift from Mary Ann Handel), 1:500; SCP1 (Abcam), 1:1500; RAD51 (Calbiochem), 1:100; RPA1 (gift from James

Ingles), 1:100; MLH1 (Santa Cruz Biotechnology), 1:100; RNF8 (gift from Xiaochun Yu), 1:100; PLZF (Calbiochem), 1:50; MRE11 (Novus), 1:200; and RAD50 (Novus), 1:200. Thereafter, slides were washed three times for 5 min in PBS plus 0.1% Tween 20, incubated with secondary antibodies (Invitrogen or Jackson ImmunoResearch) at 1:500 for 60 min in PBT, washed in PBS plus 0.1% Tween 20, and mounted in Vectashield with DAPI. The anti-BRCA1 antibody was raised in rabbits using the mouse BRCA1 fragment from 789 to 1141 amino acids (outsourced to Covance) and was used at 1:1500 dilution for immunostaining.

For double immunostaining using two primary antibodies from the same host species (mouse anti-γH2AX antibody and mouse anti-Pol II, clone 8WG), we used Fab fragments as suggested by the manufacturer (Jackson ImmunoResearch). Briefly, we first performed immunostaining of γH2AX and detected with Fab goat anti-mouse IgG conjugated with DyLight488 (Jackson ImmunoResearch). After post-fixation in 4% paraformaldehyde in PBS, we performed a second round of immunostaining with anti-RNA polymerase antibody and detection with goat anti-mouse IgG conjugated with Alexa 555 (Invitrogen). For combined RNA FISH/immunostaining, we carried out immunofluorescent detection of proteins first, followed by RNA FISH. Details of FISH and immunofluorescence microscopy are described elsewhere (Namekawa and Lee 2011).

Microarray analysis

For microarray analysis, total RNAs from whole juvenile testes at 16.5 d of age were examined on Affymetrix Gene 1.0 ST arrays. Data were analyzed using Affymetrix Expression Console software for the calculation of expression levels, with each array normalized with the RMA algorithm. Temporal expression patterns observed in genes expressed at low levels are not reliable, so low-expression probes were eliminated, as we described previously (Namekawa et al. 2006). Approximately 40% of the genes in the mouse genome are not expressed in spermatogenesis (Namekawa et al. 2006), and thus 40% of low-expression probes were eliminated prior to the analysis. For the expression analysis, probes that do not specifically annotate the genome were eliminated from the analysis. Two biological replicates were analyzed and a representative data set was shown. Excel software was used to generate the figures.

Cells; HU, siRNA, and EdU treatments; and fixation

U2OS cells were purchased from American Type Culture Collection (ATCC; HTB-96) and cultured in McCoy's 5a medium (ATCC) supplemented with 10% fetal bovine serum, penicillin, and streptomycin. For the induction of replicative stress in U2OS cells, HU (Sigma-Aldrich) was added to the medium at a final concentration of 1 mM. After 2 h of incubation with HU, cells were examined.

siRNA duplexes for Luciferase and MDC1 were designed as described previously (Galanty et al. 2009) and were obtained from Thermo Scientific. U2OS cells were transfected with siRNAs using Dharmafect 1 (Thermo Scientific). HU treatment was performed at 48 h after siRNA transfection.

EdU was added to culture medium at a final concentration of 10 μM and cells were cultured for 30 min. EdU was detected with Alexa Fluor 555 azide as suggested by the manufacturer (Invitrogen). After EdU staining, cells were further immunostained with anti-γH2AX antibodies. For the cytological analysis, cells were grown and processed on cover glasses. Cover glasses were rinsed in PBS and permeabilized with CSK buffer (100 mM NaCl, 300 mM sucrose, 10 mM PIPES at pH6.8, 3 mM $MgCl_2$) plus 0.5% Triton X-100 for 6 min on ice, followed by fixation in 4% paraformaldehyde for 10 min at room temperature. For double staining of MDC1 and γH2AX in U2OS cells, cells were fixed with −20°C cold methanol and kept for >3 h at −20°C. Cells were then washed three times with PBS and incubated in PBS with 0.5% Triton X-100 for 10 min at room temperature. After washing with PBS, cells were incubated with the following primary antibodies: γH2AX (Millipore), 1:5000; and MDC1 (AbD Serotec), 1:500.

Image acquisition and analysis

All images were acquired with a TE2000-E microscope (Nikon) and a CoolSnapHQ camera (Photometrics). All image acquisition, including *Z*-sections and deconvolution, were performed using Phylum software (Improvision). For the analysis of U2OS cells, images were captured using an Optigrid confocal system, except for immunostaining with Pol II. For immunostaining of Pol II and Cot-1 RNA FISH, *Z*-sections were captured and deconvolved with Phylum software to eliminate any secondary signals from other *Z*-sections. A representative *Z*-section was shown. Adobe Photoshop was used for composing figures. For the analysis of meiosis, we analyzed a minimum of 50 nuclei of pachytene spermatocytes per staining. Particular stages of primary spermatocytes were determined by staining for SCP3.

Acknowledgments

We thank Mary Ann Handel, Xiaochun Yu, Denise Escalier, and James Ingles for providing antibodies; Yuya Ogawa, Ho-Su Sin, and Fumika N. Hamada for discussion and helpful comments regarding the manuscript; Marina A. Bellani, Katherine Minter Dykhouse, and Margarida Almeida Santos for help in transferring mice; S. Steven Potter and Shawn Smith for help with the microarray analysis; and Erin L. Adams for editing the manuscript. S.H.N. is deeply grateful to S.K. Dey and Jeannie T. Lee for their support of the initial stage of the Namekawa laboratory. This work was supported by the Developmental Fund and Trustee Grant at Cincinnati Children's Hospital Medical Center (to S.H.N.), the NCI (NIH) Intramural Research Program (A.N.), the NIDDK (NIH) Intramural Research Program (R.D.C.-O.), and NIH grants CA130996 (to Z.L.), CA092312 (to J.C.), and HL085587 (to P.R.A.).

References

Ahmed EA, van der Vaart A, Barten A, Kal HB, Chen J, Lou Z, Minter-Dykhouse K, Bartkova J, Bartek J, de Boer P, et al. 2007. Differences in DNA double strand breaks repair in male germ cell types: lessons learned from a differential expression of Mdc1 and 53BP1. *DNA Repair (Amst)* **6:** 1243–1254.

Andreassen PR, Niedernhofer LJ. 2009. Fanconi anemia: a paradigm of discovering molecular pathways from patients. *Mutat Res* **668:** 1–3.

Baarends WM, Wassenaar E, van der Laan R, Hoogerbrugge J, Sleddens-Linkels E, Hoeijmakers JH, de Boer P, Grootegoed JA. 2005. Silencing of unpaired chromatin and histone H2A ubiquitination in mammalian meiosis. *Mol Cell Biol* **25:** 1041–1053.

Baker SM, Plug AW, Prolla TA, Bronner CE, Harris AC, Yao X, Christie DM, Monell C, Arnheim N, Bradley A, et al. 1996. Involvement of mouse Mlh1 in DNA mismatch repair and meiotic crossing over. *Nat Genet* **13:** 336–342.

Barchi M, Mahadevaiah S, Di Giacomo M, Baudat F, de Rooij DG, Burgoyne PS, Jasin M, Keeney S. 2005. Surveillance of different recombination defects in mouse spermatocytes yields distinct responses despite elimination at an identical developmental stage. *Mol Cell Biol* **25:** 7203–7215.

Baudat F, Manova K, Yuen JP, Jasin M, Keeney S. 2000. Chromosome synapsis defects and sexually dimorphic meiotic progression in mice lacking Spo11. *Mol Cell* **6:** 989–998.

Bellani MA, Romanienko PJ, Cairatti DA, Camerini-Otero RD. 2005. SPO11 is required for sex-body formation, and Spo11 heterozygosity rescues the prophase arrest of Atm−/− spermatocytes. *J Cell Sci* **118:** 3233–3245.

Burgoyne PS, Mahadevaiah SK, Turner JM. 2009. The consequences of asynapsis for mammalian meiosis. *Nat Rev Genet* **10:** 207–216.

Carrel L, Willard HF. 2005. X-inactivation profile reveals extensive variability in X-linked gene expression in females. *Nature* **434:** 400–404.

Celeste A, Petersen S, Romanienko PJ, Fernandez-Capetillo O, Chen HT, Sedelnikova OA, Reina-San-Martin B, Coppola V, Meffre E, Difilippantonio MJ, et al. 2002. Genomic instability in mice lacking histone H2AX. *Science* **296:** 922–927.

Celeste A, Fernandez-Capetillo O, Kruhlak MJ, Pilch DR, Staudt DW, Lee A, Bonner RF, Bonner WM, Nussenzweig A. 2003. Histone H2AX phosphorylation is dispensable for the initial recognition of DNA breaks. *Nat Cell Biol* **5:** 675–679.

Chaumeil J, Le Baccon P, Wutz A, Heard E. 2006. A novel role for Xist RNA in the formation of a repressive nuclear compartment into which genes are recruited when silenced. *Genes Dev* **20:** 2223–2237.

Chow JC, Heard E. 2010. Nuclear organization and dosage compensation. *Cold Spring Harb Perspect Biol* **2:** a000604. doi: 10.1101/cshperspect.a000604.

Cimprich KA, Cortez D. 2008. ATR: an essential regulator of genome integrity. *Nat Rev Mol Cell Biol* **9:** 616–627.

Eijpe M, Offenberg H, Goedecke W, Heyting C. 2000. Localisation of RAD50 and MRE11 in spermatocyte nuclei of mouse and rat. *Chromosoma* **109:** 123–132.

Escalier D, Garchon HJ. 2000. XMR is associated with the asynapsed segments of sex chromosomes in the XY body of mouse primary spermatocytes. *Chromosoma* **109:** 259–265.

Fernandez-Capetillo O, Mahadevaiah SK, Celeste A, Romanienko PJ, Camerini-Otero RD, Bonner WM, Manova K, Burgoyne P, Nussenzweig A. 2003. H2AX is required for chromatin remodeling and inactivation of sex chromosomes in male mouse meiosis. *Dev Cell* **4:** 497–508.

Friedel AM, Pike BL, Gasser SM. 2009. ATR/Mec1: coordinating fork stability and repair. *Curr Opin Cell Biol* **21:** 237–244.

Furuta T, Takemura H, Liao ZY, Aune GJ, Redon C, Sedelnikova OA, Pilch DR, Rogakou EP, Celeste A, Chen HT, et al. 2003. Phosphorylation of histone H2AX and activation of Mre11, Rad50, and Nbs1 in response to replication-dependent DNA double-strand breaks induced by mammalian DNA topoisomerase I cleavage complexes. *J Biol Chem* **278:** 20303–20312.

Galanty Y, Belotserkovskaya R, Coates J, Polo S, Miller KM, Jackson SP. 2009. Mammalian SUMO E3-ligases PIAS1 and PIAS4 promote responses to DNA double-strand breaks. *Nature* **462:** 935–939.

Goldberg M, Stucki M, Falck J, D'Amours D, Rahman D, Pappin D, Bartek J, Jackson SP. 2003. MDC1 is required for the intra-S-phase DNA damage checkpoint. *Nature* **421:** 952–956.

Greaves IK, Rangasamy D, Devoy M, Marshall Graves JA, Tremethick DJ. 2006. The X and Y chromosomes assemble into H2A.Z, containing facultative heterochromatin, following meiosis. *Mol Cell Biol* **26:** 5394–5405.

Hall LL, Byron M, Sakai K, Carrel L, Willard HF, Lawrence JB. 2002. An ectopic human XIST gene can induce chromosome inactivation in postdifferentiation human HT-1080 cells. *Proc Natl Acad Sci* **99:** 8677–8682.

Hoyer-Fender S, Costanzi C, Pehrson JR. 2000. Histone macroH2A1.2 is concentrated in the XY-body by the early pachytene stage of spermatogenesis. *Exp Cell Res* **258:** 254–260.

Huen MS, Grant R, Manke I, Minn K, Yu X, Yaffe MB, Chen J. 2007. RNF8 transduces the DNA-damage signal via histone ubiquitylation and checkpoint protein assembly. *Cell* **131:** 901–914.

Huen MS, Sy SM, Chen J. 2010. BRCA1 and its toolbox for the maintenance of genome integrity. *Nat Rev Mol Cell Biol* **11:** 138–148.

Huynh KD, Lee JT. 2005. X-chromosome inactivation: a hypothesis linking ontogeny and phylogeny. *Nat Rev Genet* **6:** 410–418.

Inagaki A, Schoenmakers S, Baarends WM. 2010. DNA double strand break repair, chromosome synapsis and transcriptional silencing in meiosis. *Epigenetics* **5:** 255–266.

Inselman A, Eaker S, Handel MA. 2003. Temporal expression of cell cycle-related proteins during spermatogenesis: establishing a timeline for onset of the meiotic divisions. *Cytogenet Genome Res* **103:** 277–284.

Kelly WG, Aramayo R. 2007. Meiotic silencing and the epigenetics of sex. *Chromosome Res* **15:** 633–651.

Kolas NK, Chapman JR, Nakada S, Ylanko J, Chahwan R, Sweeney FD, Panier S, Mendez M, Wildenhain J, Thomson TM, et al. 2007. Orchestration of the DNA-damage response by the RNF8 ubiquitin ligase. *Science* **318:** 1637–1640.

Lee JT. 2010. The X as model for RNA's niche in epigenomic regulation. *Cold Spring Harb Perspect Biol* **2:** a003749. doi: 10.1101/cshperspect.a003749.

Lee AC, Fernandez-Capetillo O, Pisupati V, Jackson SP, Nussenzweig A. 2005. Specific association of mouse MDC1/NFBD1 with NBS1 at sites of DNA-damage. *Cell Cycle* **4:** 177–182.

Lou Z, Minter-Dykhouse K, Wu X, Chen J. 2003. MDC1 is coupled to activated CHK2 in mammalian DNA damage response pathways. *Nature* **421:** 957–961.

Lou Z, Minter-Dykhouse K, Franco S, Gostissa M, Rivera MA, Celeste A, Manis JP, van Deursen J, Nussenzweig A, Paull TT, et al. 2006. MDC1 maintains genomic stability by participating in the amplification of ATM-dependent DNA damage signals. *Mol Cell* **21:** 187–200.

Lu LY, Wu J, Ye L, Gavrilina GB, Saunders TL, Yu X. 2010. RNF8-dependent histone modifications regulate nucleosome removal during spermatogenesis. *Dev Cell* **18:** 371–384.

Mahadevaiah SK, Turner JM, Baudat F, Rogakou EP, de Boer P, Blanco-Rodriguez J, Jasin M, Keeney S, Bonner WM, Burgoyne PS. 2001. Recombinational DNA double-strand breaks in mice precede synapsis. *Nat Genet* **27:** 271–276.

Mahadevaiah SK, Bourc'his D, de Rooij DG, Bestor TH, Turner JM, Burgoyne PS. 2008. Extensive meiotic asynapsis in mice antagonises meiotic silencing of unsynapsed chromatin and consequently disrupts meiotic sex chromosome inactivation. *J Cell Biol* **182:** 263–276.

Mailand N, Bekker-Jensen S, Faustrup H, Melander F, Bartek J, Lukas C, Lukas J. 2007. RNF8 ubiquitylates histones at DNA double-strand breaks and promotes assembly of repair proteins. *Cell* **131:** 887–900.

McCarrey JR, Watson C, Atencio J, Ostermeier GC, Marahrens Y, Jaenisch R, Krawetz SA. 2002. X-chromosome inactivation during spermatogenesis is regulated by an Xist/Tsix-independent mechanism in the mouse. *Genesis* **34:** 257–266.

McKee BD, Handel MA. 1993. Sex chromosomes, recombination, and chromatin conformation. *Chromosoma* **102:** 71–80.

Moens PB, Tarsounas M, Morita T, Habu T, Rottinghaus ST, Freire R, Jackson SP, Barlow C, Wynshaw-Boris A. 1999. The association of ATR protein with mouse meiotic chromosome cores. *Chromosoma* **108:** 95–102.

Namekawa SH, Lee JT. 2009. XY and ZW: is meiotic sex chromosome inactivation the rule in evolution? *PLoS Genet* **5:** e1000493. doi: 10.1371/journal.pgen.1000493.

Namekawa SH, Lee JT. 2011. Detection of nascent RNA, single-copy DNA and protein localization by immunoFISH in murine germ cells and pre-implantation embryos. *Nat Protoc* **6:** 270–284.

Namekawa SH, Park PJ, Zhang LF, Shima JE, McCarrey JR, Griswold MD, Lee JT. 2006. Postmeiotic sex chromatin in the male germline of mice. *Curr Biol* **16:** 660–667.

Namekawa SH, VandeBerg JL, McCarrey JR, Lee JT. 2007. Sex chromosome silencing in the marsupial male germ line. *Proc Natl Acad Sci* **104:** 9730–9735.

Namekawa SH, Payer B, Huynh KD, Jaenisch R, Lee JT. 2010. Two-step imprinted X inactivation: repeat versus genic silencing in the mouse. *Mol Cell Biol* **30:** 3187–3205.

Okamoto I, Otte AP, Allis CD, Reinberg D, Heard E. 2004. Epigenetic dynamics of imprinted X inactivation during early mouse development. *Science* **303:** 644–649.

Perera D, Perez-Hidalgo L, Moens PB, Reini K, Lakin N, Syvaoja JE, San-Segundo PA, Freire R. 2004. TopBP1 and ATR colocalization at meiotic chromosomes: role of TopBP1/Cut5 in the meiotic recombination checkpoint. *Mol Biol Cell* **15:** 1568–1579.

Peters AH, Plug AW, van Vugt MJ, de Boer P. 1997. A drying-down technique for the spreading of mammalian meiocytes from the male and female germline. *Chromosome Res* **5:** 66–68.

Plug AW, Peters AH, Keegan KS, Hoekstra MF, de Boer P, Ashley T. 1998. Changes in protein composition of meiotic nodules during mammalian meiosis. *J Cell Sci* **111:** 413–423.

Reini K, Uitto L, Perera D, Moens PB, Freire R, Syvaoja JE. 2004. TopBP1 localises to centrosomes in mitosis and to chromosome cores in meiosis. *Chromosoma* **112:** 323–330.

Rogers RS, Inselman A, Handel MA, Matunis MJ. 2004. SUMO modified proteins localize to the XY body of pachytene spermatocytes. *Chromosoma* **113:** 233–243.

Romanienko PJ, Camerini-Otero RD. 2000. The mouse Spo11 gene is required for meiotic chromosome synapsis. *Mol Cell* **6:** 975–987.

Santos MA, Huen MS, Jankovic M, Chen HT, Lopez-Contreras AJ, Klein IA, Wong N, Barbancho JL, Fernandez-Capetillo O, Nussenzweig MC, et al. 2010. Class switching and meiotic defects in mice lacking the E3 ubiquitin ligase RNF8. *J Exp Med* **207:** 973–981.

Scully R, Chen J, Plug A, Xiao Y, Weaver D, Feunteun J, Ashley T, Livingston DM. 1997. Association of BRCA1 with Rad51 in mitotic and meiotic cells. *Cell* **88:** 265–275.

Shanbhag NM, Rafalska-Metcalf IU, Balane-Bolivar C, Janicki SM, Greenberg RA. 2010. ATM-dependent chromatin changes silence transcription in cis to DNA double-strand breaks. *Cell* **141:** 970–981.

Song R, Ro S, Michaels JD, Park C, McCarrey JR, Yan W. 2009. Many X-linked microRNAs escape meiotic sex chromosome inactivation. *Nat Genet* **41:** 488–493.

Stewart GS, Wang B, Bignell CR, Taylor AM, Elledge SJ. 2003. MDC1 is a mediator of the mammalian DNA damage checkpoint. *Nature* **421:** 961–966.

Tarsounas M, Morita T, Pearlman RE, Moens PB. 1999. RAD51 and DMC1 form mixed complexes associated with mouse meiotic chromosome cores and synaptonemal complexes. *J Cell Biol* **147:** 207–220.

Turner JM. 2007. Meiotic sex chromosome inactivation. *Development* **134:** 1823–1831.

Turner JM, Mahadevaiah SK, Elliott DJ, Garchon HJ, Pehrson JR, Jaenisch R, Burgoyne PS. 2002. Meiotic sex chromosome inactivation in male mice with targeted disruptions of Xist. *J Cell Sci* **115:** 4097–4105.

Turner JM, Aprelikova O, Xu X, Wang R, Kim S, Chandramouli GV, Barrett JC, Burgoyne PS, Deng CX. 2004. BRCA1, histone H2AX phosphorylation, and male meiotic sex chromosome inactivation. *Curr Biol* **14:** 2135–2142.

Turner JM, Mahadevaiah SK, Fernandez-Capetillo O, Nussenzweig A, Xu X, Deng CX, Burgoyne PS. 2005. Silencing of unsynapsed meiotic chromosomes in the mouse. *Nat Genet* **37:** 41–47.

Turner JM, Mahadevaiah SK, Ellis PJ, Mitchell MJ, Burgoyne PS. 2006. Pachytene asynapsis drives meiotic sex chromosome inactivation and leads to substantial postmeiotic repression in spermatids. *Dev Cell* **10:** 521–529.

van der Heijden GW, Derijck AA, Posfai E, Giele M, Pelczar P, Ramos L, Wansink DG, van der Vlag J, Peters AH, de Boer P. 2007. Chromosome-wide nucleosome replacement and H3.3 incorporation during mammalian meiotic sex chromosome inactivation. *Nat Genet* **39:** 251–258.

Vigodner M. 2009. Sumoylation precedes accumulation of phosphorylated H2AX on sex chromosomes during their meiotic inactivation. *Chromosome Res* **17:** 37–45.

Wang J, Gong Z, Chen J. 2011. MDC1 collaborates with TopBP1 in DNA replication checkpoint control. *J Cell Biol* doi: 10.1083/jcb.201010026.

Yamane K, Wu X, Chen J. 2002. A DNA damage-regulated BRCT-containing protein, TopBP1, is required for cell survival. *Mol Cell Biol* **22:** 555–566.

Yan W, McCarrey JR. 2009. Sex chromosome inactivation in the male. *Epigenetics* **4:** 452–456.